

CHROME: Clothed Human Reconstruction with Occlusion-Resilience and Multiview-Consistency from a Single Image

Arindam Dutta¹ Meng Zheng² Zhongpai Gao² Benjamin Planche² Anwasha Choudhuri²
 Terrence Chen² Amit K. Roy-Chowdhury¹ Ziyang Wu²

¹University of California, Riverside

²United Imaging Intelligence, Boston

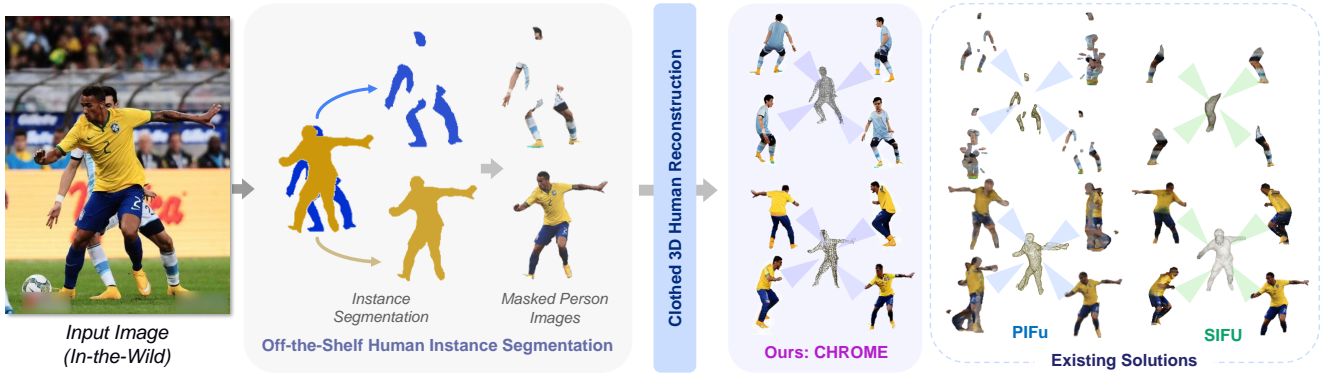


Figure 1. **Need for occlusion-resilient multiview-consistent clothed human reconstruction from single images:** Existing algorithms for monocular 3D clothed human reconstruction, such as PIFu [1] and SIFU [2], produce fragmented and multiview-inconsistent novel view reconstructions from single-view occluded human images [3]. In contrast, CHROME generates occlusion-free, multiview-consistent novel views from a single occluded image, using a novel pose-controlled multiview diffusion model, combined with a large reconstruction model, to create a cohesive 3D representation of the human subject. Moreover, CHROME does not require 3D mesh supervision during training as required for existing algorithms [1, 2].

Abstract

Reconstructing clothed humans from a single image is a fundamental task in computer vision with wide-ranging applications. Although existing monocular clothed human reconstruction solutions have shown promising results, they often rely on the assumption that the human subject is in an occlusion-free environment. Thus, when encountering in-the-wild occluded images, these algorithms produce multiview inconsistent and fragmented reconstructions. Additionally, most algorithms for monocular 3D human reconstruction leverage geometric priors such as SMPL annotations for training and inference, which are extremely challenging to acquire in real-world applications. To address these limitations, we propose CHROME: Clothed Human Reconstruction with Occlusion-Resilience and Multiview-Consistency from a Single Image, a novel pipeline designed to reconstruct occlusion-resilient 3D humans with multiview consistency from a single occluded image, without requiring either ground-truth geometric prior annotations or

3D supervision. Specifically, CHROME leverages a multiview diffusion model to first synthesize occlusion-free human images from the occluded input, compatible with off-the-shelf pose control to explicitly enforce cross-view consistency during synthesis. A 3D reconstruction model is then trained to predict a set of 3D Gaussians conditioned on both the occluded input and synthesized views, aligning cross-view details to produce a cohesive and accurate 3D representation. CHROME achieves significant improvements in terms of both novel view synthesis (upto 3 db PSNR) and geometric reconstruction under challenging conditions.

1. Introduction

The task of reconstructing a 3D clothed human reconstruction involves generating a 3D human model from multiview images [4] or monocular videos [5] with numerous applications spanning augmented reality, virtual try-on and digital avatars [6, 7]. However, these approaches are often impractical as capturing multiview images in real-world settings is neither budget-friendly nor scalable. This lim-

itation has driven researchers to focus on *single-view 3D clothed human reconstruction* algorithms, which encompasses reconstructing a 3D human model from just a single image [1, 2, 8–10]. However, *occlusions remain a major obstacle, often resulting in fragmented and inaccurate multi-view reconstructions* [11, 12], making existing approaches impractical for real world settings. Although recent studies have improved occlusion resilience for specific low-level human modeling tasks such as segmentation [13] and pose estimation [14, 15], **reconstructing occlusion-resilient and multi-view consistent** texture and 3D geometric details from novel camera views under occlusion remains largely unaddressed. As visualized in Figure 1, existing algorithms for single-view 3D clothed human reconstruction [1, 2] perform poorly in in-the-wild scenarios when the human subject is partially occluded, resulting in inconsistent and fragmented novel view synthesis.

Existing 3D clothed human reconstruction methods can be divided into several main streams based on different volumetric representations, traditional 3D human reconstruction learns parametric models such as SMPL [16], which show moderate occlusion resilience by embedding human body priors but prioritize surface reconstruction over texture [17, 18], with limited appearance detail for clothed human reconstruction. However, these methods typically require large-scale image and SMPL pose/shape pairs for training, which demands labor-intensive annotation and often compromises generalizability under in-the-wild scenes. On the other hand, implicit representations like Neural Radiance Fields (NeRFs) [5, 19] and point-based representations like 3D Gaussian Splatting (3DGS) [20, 21] offer high visual-fidelity human reconstruction from monocular videos. However, they struggle with occlusions as they often require pixel-level fine details for subject-specific optimization, which can be largely affected by occlusion noises, as discussed in [12, 22].

To address these challenges, we propose **CHROME: Clothed Human Reconstruction with Occlusion-Resilience and Multiview-Consistency**, which leverages a multiview diffusion model to generate consistent, occlusion-free multiview human images to learn a 3D Gaussian representation from occluded monocular image input. Specifically CHROME adopts a two-stage learning strategy. In the first stage, CHROME addresses the limited information available in a single-view occluded image using a multiview diffusion model [23], compatible with off-the-shelf pose control, to generate four occlusion-free cross-view consistent human images. Using an estimated 3D pose as an explicit guidance signal, we ensure enhanced pose consistency across the generated views, which is essential for a coherent 3D human representation. The second stage of CHROME incorporates a 3D reconstruction model that learns to predict a set of 3D Gaussians [20], providing a cohesive 3D representation

of the human subject. This model is conditioned on both the initial occluded image and the synthesized multiview occlusion-free images, enabling it to capture and integrate geometric and texture details consistently across views.

The proposed two-stage approach effectively bridges 2D-3D information gaps, advancing the capability of single-image-based 3D reconstruction under occlusions. On the other hand, by optimizing the photometric loss in the 2D projected space CHROME is able to take advantage of large-scale 2D human images for implicit geometric prior learning, eliminating the need to require 3D supervision and SMPL priors as in existing solutions [1, 2, 9, 10, 24], resulting in superior generalizability under occlusions in real-world application scenarios.

The following are the main contributions of the work.

- We address the problem of multiview reconstruction of a human subject under occlusions from a single view image. This addresses the bottlenecks associated with existing algorithms, which perform poorly under occlusions.
- To tackle the aforementioned problem, we propose CHROME, a novel algorithm that utilizes a multiview diffusion model, enabling off-the-shelf pose control to generate cross-view de-occluded images from a single occluded input. A reconstruction model then predicts a cohesive set of 3D Gaussians conditioned on both the occluded input and the synthesized views, enabling occlusion-free novel view synthesis.
- CHROME does not require ground-truth SMPL mesh annotations as in existing algorithms. We further demonstrate the generalizability of the proposed pipeline with stereo input with improved reconstruction accuracy and cross-view consistency.
- Extensive experiments showcase the strength of CHROME in novel view synthesis from a single occluded human image in both in-domain and zero-shot settings.

2. Related Works

Monocular Human Mesh Recovery: Monocular Human Mesh Recovery aims to generate a 3D human mesh from a single image [25], predominantly using the SMPL model [26] and its variants for 3D pose and shape estimation. Recent advances [27–30] have leveraged large-scale synthetic [31] and real-world datasets [32–34], improving reconstruction for diverse datasets and in-the-wild scenarios [35]. However, challenges remain in handling occlusions, with recent methods [36–38] focusing on occlusion-robust algorithms often using learned priors like [39, 40] to enhance reconstruction reliability. Despite these advancements, these algorithms focus primarily on bare-body mesh recovery, often overlooking the challenges of reconstructing texture and clothing details.

Clothed Human Reconstruction: Clothed human reconstruction focuses on generating a 3D mesh of clothed sub-

jects, textured or untextured, from various inputs such as single images, multiview images, or monocular videos. Existing methods fall primarily into two categories: implicit function-based techniques [1, 2, 9, 10, 17, 18, 24] and rendering-based approaches [5, 21, 41, 42]. Implicit function-based methods, such as PIFu [1] and its extensions [8], leverage pixel-aligned features processed through learnable decoders to reconstruct detailed 3D models using 3D supervision. Recent approaches like GTA [9] and SIFU [2] incorporate the SMPL model to embed anatomical priors, improving the fidelity of reconstruction. TeCH [43] applies optimization techniques to achieve single-image 3D digitization. However, occlusions persist as a critical challenge in clothed human reconstruction. Wang *et al.* [44] proposed a methodology utilizing ground-truth SMPL meshes to mitigate occlusion effects. However, their framework presents two principal limitations: heavy reliance on precise SMPL mesh estimations, which are inherently challenging to acquire under occluded conditions, and lack of publicly available codes, obstructing both reproducibility and practical adoption. With advances in Neural Radiance Fields (NeRFs) [19] and 3D Gaussian Splatting (3DGS) [20], studies such as [5, 21] have adapted these techniques for human reconstruction from monocular videos, though occlusion handling remains problematic, as evidenced in occlusion-robust variants [12, 22, 45]. Despite this progress, they typically require monocular video inputs and are optimized per subject, limiting their scalability and practical deployment. Differently, we propose a single image-based generalizable approach for occlusion-free novel view synthesis and geometric reconstruction.

Multi-view Diffusion and Large Reconstruction Models for 3D Reconstruction: Latent Diffusion Models (LDMs) [46] have aided significant advancements in image generation, reconstruction, and single-image-to-3D tasks. Zero-1-to-3 [47] pioneered the use of LDMs to generate novel views from single input images with specified camera parameters, sparking a wave of related research [23, 48–50]. ControlNet [51] introduced guided control over LDM sampling, advancing conditional generation. Recent works facilitate the creation of 3D objects from text prompts [52, 53] by leveraging extensive training datasets [54]. Pretrained LDMs also function as priors for novel view synthesis, modeling natural image distributions, and penalizing the reconstruction model through Score Distillation Sampling based losses [55–57]. Recently, the Large Reconstruction Model (LRM) [58] introduced NeRF-based triplane representations for efficient single image to 3D generation, trained on large multiview datasets [59, 60]. Large Gaussian Model (LGM) [61] extended the same by integrating pretrained diffusion models for single-image-to-3D synthesis, achieving faster rendering with 3DGS techniques. However, these algorithms struggle with partial occlusions, mo-

tivating our proposed approach for 3D human recovery from single or stereo occluded images.

3. Methodology

In this section, we introduce our proposed algorithm CHROME, which is designed to generate occlusion-free novel views of a human subject from a single image, where the subject can be partially obscured by occlusions. Specifically, given an input image $x \in \mathbb{R}^{H \times W \times 3}$, representing a partially visible human subject within spatial dimensions H and W , CHROME reconstructs N occlusion-free novel views (denoted as $y \in \mathbb{R}^{N \times H \times W \times 3}$) of this subject. Additionally, while we use a single-view image as input for clearer illustration, it is important to note that our pipeline is fully compatible with multiview inputs.

The pipeline CHROME is structured with two distinct modules and is trained from end-to-end to achieve novel view synthesis from a single occluded image x . The first module, \mathcal{F}_D , leverages the power of latent diffusion models [46] in conjunction with ControlNet [51] to synthesize four pose-controlled, multiview-consistent images from the occluded input. These occlusion-free images form the basis for novel synthesis under occluded single-view inputs. The second module, \mathcal{F}_R , learns to reconstruct occlusion-free views by combining information from both the original occluded input and the \mathcal{F}_D generated images. This results in N occlusion-free novel views of the human subject.

$$y = \mathcal{F}_R \circ \mathcal{F}_D(x), \quad (1)$$

where the composition of functions \mathcal{F}_R and \mathcal{F}_D denotes the sequential application of the diffusion and reconstruction modules. The complete architecture of the proposed algorithm, CHROME, is depicted in Figure 2.

3.1. Pose Controlled Multiview Consistent Diffusion

Given a single occluded image x , the objective of \mathcal{F}_D is to generate four pose-controlled, multiview consistent images, represented by $y_D \in \mathbb{R}^{4 \times H \times W \times 3}$. Each of these images in y_D corresponds to a unique view, achieved by rotating the camera around a fixed radius at angles of 0° , 90° , 180° , and 270° . We employ a latent diffusion model (LDM) [46] to define \mathcal{F}_D , allowing it to learn the conditional distribution of these four multiview images based on the occluded input image. The denoising diffusion process operates within the latent space of \mathcal{F}_D leveraging a pretrained variational autoencoder (VAE) that efficiently encodes and decodes latent vectors for image reconstruction.

The task of reconstructing multiview images based on a single occluded image is inherently ill-posed and under-constrained, making it essential to introduce suitable conditions to regularize the learning process. To address this, we employ a pre-trained VAE encoder module, \mathcal{E} , to extract features from the visible regions of x , which are then

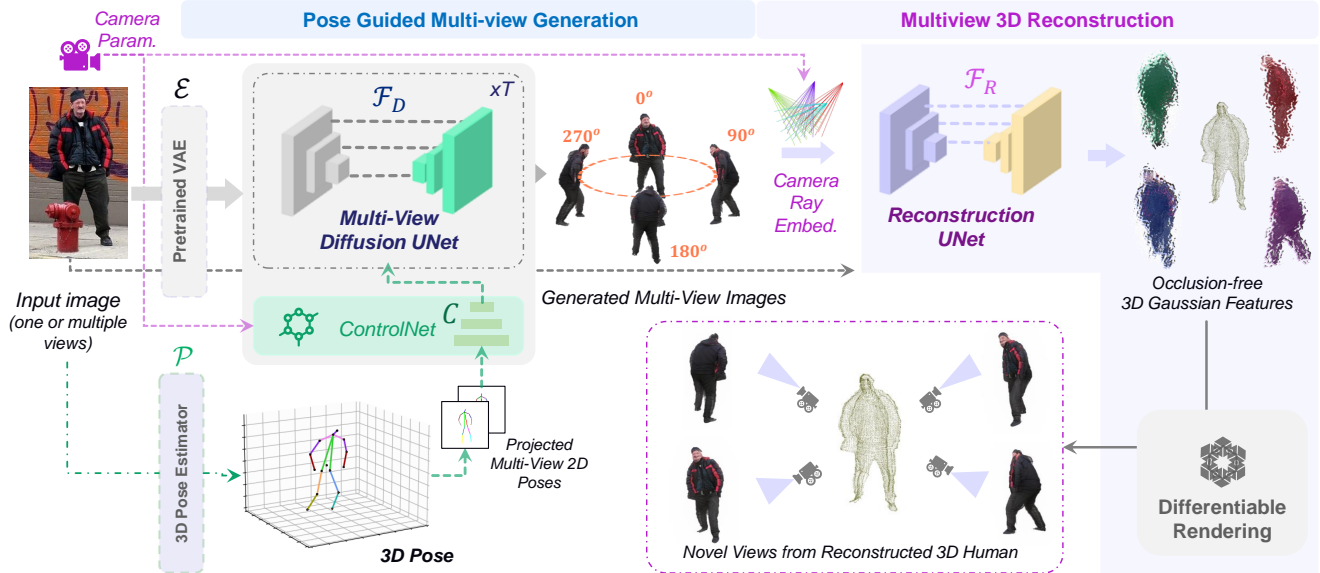


Figure 2. **Overview of proposed method:** CHROME is a novel two-stage pipeline designed for occlusion-free 3D human reconstruction from a single occluded image. In the first stage, a pose-controlled multiview diffusion model generates four de-occluded views of the subject, ensuring pose consistency across the synthesized images, conditioned on the input occluded image and the 3D pose estimates. In the second stage, a 3D reconstruction model combines the occluded input image with the synthesized multi-view images to create a cohesive 3D Gaussian representation, aligning geometric and texture details across views, enabling accurate reconstructions and robust novel view synthesis, even in the presence of significant occlusions. Note that the method is also compatible with multi-view inputs.

passed on to \mathcal{F}_D . This step ensures conditioning the multiview generation on the observable portions of x , ensuring that the output images maintain a consistent appearance with the visible parts of the occluded input image. However, we observe that multiview image generation with conditioning \mathcal{F}_D solely on occluded input image features sometimes results in multiview images with suboptimal cross-view consistency. Hence, we utilize a ControlNet [51] (\mathcal{C}) based approach to explicitly condition the diffusion process on the 2D target poses (\mathbf{P}_D^{2d}), ensuring pose consistency across generated multiview images. This strategy further regularizes \mathcal{F}_D , guiding it to produce consistent multiview pose-aligned output images.

To train the model \mathcal{F}_D , we first generate paired input and multiview target images with camera orientations set at 0° , 90° , 180° , and 270° relative to the camera parameters of the input image, using rendered images from \mathcal{S} . Following the approach of [62], random occlusions are applied to the input images, resulting in paired occluded input images x and corresponding ground-truth multiview target images y_D . The ground-truth latent vector is defined as $z_0 = \mathcal{E}(y_D)$ and undergoes perturbation through the diffusion process across t timesteps to produce z_t . The objective of \mathcal{F}_D is to recover the perturbation noise $\epsilon_{\mathcal{F}_D}$ at each timestep t , conditioned on features from the occluded input image $\mathcal{E}(x)$ and a control signal provided by the ground-truth 2D target poses through ControlNet, denoted as $\mathcal{C}(\mathbf{P}_D^{2d})$. Thus, the

training objective can be formally expressed as

$$\min_{\mathcal{F}_D} \mathbb{E}_{z \sim \mathcal{E}(x), t, \epsilon \sim \mathcal{N}(0, I)} \|\epsilon - \epsilon_{\mathcal{F}_D}(z_t; t, \mathcal{E}(x), \mathcal{C}(\mathbf{P}_D^{2d}))\|_2^2. \quad (2)$$

Furthermore, since diffusion models generally require large-scale training data to achieve effective convergence, we follow prior work [10, 63] by initializing \mathcal{F}_D with pre-trained weights from [23], which was trained on an extensive collection of multiview images from [59]. In our training, we fine-tune only the parameters of the UNet [46] and ControlNet [51] models, leaving all other parameters, including the encoder and decoder of the VAE fixed. Furthermore, by conditioning \mathcal{F}_D on the features of the input image $\mathcal{E}(x)$, we ensure that even under incorrect pose predictions, y_D retains the information in the original input image x (see the supplementary for more discussion).

During the inference phase, we employ a state-of-the-art 3D pose estimation model, \mathcal{P} [35], to estimate the 3D pose, denoted as $\hat{\mathbf{P}}^{3d}$, of the human subject from the occluded image input x . This extraction is represented by $\hat{\mathbf{P}}^{3d} = \mathcal{P}(x)$. Using a weak-perspective projection, we then obtain the corresponding 2D pose $\hat{\mathbf{P}}_D^{2d}$ for each multiview image. To generate the estimated multiview images \hat{y}_D , we utilize the pretrained VAE decoder module, \mathcal{D} , applied on the denoised latent vector \hat{z}_0 which is acquired through an iterative DDIM denoising (sampling) process [64] over T timesteps, beginning from Gaussian noise and conditioned on both the occluded input image embedding $\mathcal{E}(x)$ and the

estimated multiview 2D pose conditioning $\mathcal{C}(\hat{\mathbf{P}}_D^{2d})$. Mathematically, $\hat{y}_D = \mathcal{D}(\hat{z}_0)$. Figure 3 shows the qualitative results of our \mathcal{F}_D in generating occlusion free novel views conditioned on the occluded input image.

3.2. Novel View Synthesis using Gaussian Splatting

To achieve an occlusion-free 3D representation of the human subject using the four multiview images produced by our proposed pose-controlled multiview diffusion model, we build upon recent advancements in 3D Gaussian Splatting [20]. Specifically, our aim is to use the synthesized multiview images, generated by our diffusion function \mathcal{F}_D , alongside the original occluded input image, denoted x , to inform a learning framework that maps this set of images to a 3D Gaussian representation. This mapping (\mathcal{F}_R) facilitates the transition from a spatially diverse image array to a continuous Gaussian field that approximates the underlying human subject in 3D space.

Formally, we define \mathcal{F}_R as a transformation that operates on a tensor of five images, each of dimensions $H \times W$ and containing RGB values, such that $\mathcal{F}_R : \mathbb{R}^{5 \times H \times W \times 3} \rightarrow \mathbb{R}^{n_g \times 14}$, where n_g denotes the number of Gaussians representing the human subject. Each Gaussian is represented by a precise set of parameters: mean $\in \mathbb{R}^3$, scaling $\in \mathbb{R}^3$, rotation quaternion $\in \mathbb{R}^4$, opacity value $\in \mathbb{R}$, and colors $\in \mathbb{R}^3$. Together, these elements constitute a 14-dimensional vector that encapsulates both spatial and appearance information essential for Gaussian representation. This compact representation supports efficient computation while preserving essential structural and visual details in the 3D space. By aligning these Gaussian representations across the multiview images, we achieve a cohesive occlusion-resilient 3D model of the underlying human subject.

To model the function \mathcal{F}_R , we employ an asymmetric UNet architecture [61] specifically designed to incorporate information from both the occluded input image and the synthesized multiview images. This architecture enables a seamless fusion of spatial and appearance details, ensuring a holistic 3D representation. Following the approach outlined in [65], we encode camera poses into a 9-channel feature map, combining RGB values with ray embeddings to produce a unified representation that integrates color and spatial orientation for input to \mathcal{F}_R . Drawing inspiration from [66], we treat each pixel in the resulting output feature map as an individual 3D Gaussian, forming a continuous Gaussian field that effectively captures both local details and spatial coherence. The final 3D Gaussian representation is achieved by concatenating the output Gaussians from each view, which are then rendered at the target resolution for supervision for generating multiview images.

To supervise the learning of \mathcal{F}_R , we utilize a differentiable renderer [20] that projects the final 3D Gaussian representation into a set of multiview images based on prede-

finied camera parameters. Specifically, N multiview images, denoted as $\{\hat{y}_i\}_{i=1}^N$, are generated from the final 3D Gaussian representation. These rendered images are then used to compute a combined loss function, encompassing photometric loss in the rendered RGB images and shape loss in the rendered α image [20] and the ground truth silhouettes $\{y_{silh}^{gt}\}_{i=1}^N$, with respect to the ground truth multiview images $\{y_i^{gt}\}_{i=1}^N$, which guide the optimization of \mathcal{F}_R . The objective function is formulated as follows:

$$\min_{\mathcal{F}_R} \mathcal{L}_{\text{mse}}(\hat{y}, y^{\text{gt}}) + \lambda_1 \mathcal{L}_{\text{lpips}}(\hat{y}, y^{\text{gt}}) + \lambda_2 \mathcal{L}_{\text{mse}}(\hat{y}_\alpha, y_{silh}^{\text{gt}}) \quad (3)$$

The weights λ_1 and λ_2 control the relative influence of each term in the objective function, and \mathcal{L}_{mse} represents the mean squared error loss, $\mathcal{L}_{\text{lpips}}$ is the perceptual loss [67]. Additionally, during CHROME’s end-to-end training, we enable *estimated* 3D pose control derived from occluded images instead of ground-truth poses, which enhances CHROME’s generalizability and robustness in real-world scenarios where perfect pose information is not available.

To enable learning of \mathcal{F}_D and \mathcal{F}_R , we utilize a dataset \mathcal{S} [68] consisting of textured human scans. For each scan, we render the corresponding images by positioning 16 equidistant perspective cameras at a fixed elevation, scene radius, and focal lengths, following the setup in [4]. During inference, given an occluded image x , we first compute synthetic occlusion-free images as $\hat{y}_D = \mathcal{F}_D(x)$. Next, the concatenated input $[x; \hat{y}_D]$ is passed through \mathcal{F}_R to generate N novel view images, denoted by $\{\hat{y}_i\}_{i=1}^N$, which can be mathematically expressed as $\{\hat{y}_i\}_{i=1}^N = \mathcal{F}_R([x; \hat{y}_D])$

4. Experiments and Results

In this section, we demonstrate CHROME’s outstanding ability to perform occlusion-free novel view synthesis and geometric reconstruction for single-view occluded human image on multiple datasets, presenting both qualitative and quantitative analyses on multiple benchmarks.

Datasets: We evaluate our method on multiple datasets: THuman2.0 [68] (526 high-quality scans of 150 clothing styles across 500 training and 26 evaluation subjects) using a perspective camera (49.1° FOV) with 16 views per subject; CustomHumans [69] containing 600 scans of 80 subjects with 120 garments, augmented with artificial occlusions for zero-shot testing; CAPE [70] containing 15 subjects in tight clothing, modified with synthetic occlusions for zero-shot evaluation and AHP [11] featuring naturally occluded in-the-wild images used for input-view de-occlusion assessment.

Implementation details: For all our experiments, we use the PyTorch coding environment with all models being



Figure 3. **Qualitative analysis of \mathcal{F}_D in generating occlusion-free novel views:** Qualitative results demonstrating the capacity of \mathcal{F}_D in generating occlusion-free novel views conditioned on a single occluded image from CustomHumans (left) and AHP (right).

trained on $4 \times$ A40 GPUs. We train \mathcal{F}_D for 100 epochs across all experiments. The training utilizes the AdamW optimizer with a cosine annealing learning rate schedule that peaks at 7×10^{-5} within 1000 warm-up steps, after which we use a constant learning rate of 5×10^{-6} . During inference, we employ classifier-free guidance with a guidance scale of 4 and 40 diffusion steps, utilizing an ancestral Euler sampling strategy. For training \mathcal{F}_R , we use a learning rate initialized at 4×10^{-4} , which decays following the Cosine Annealing strategy over 100 epochs. In Equation 4 (see main paper), λ_1 is set to 1.5 and λ_2 is set to 1.

Metrics: We follow [1, 2, 9] and use PSNR, SSIM [71], and LPIPS [67] to evaluate reconstruction accuracy in 2D and chamfer distance (CD) in cm, point-to-surface (P2S) error (cm), and normal consistency (NC) [10] to evaluate 3D reconstruction quality.

Table 1. Quantitative comparison for Novel View Texture Reconstruction on Occluded THuman2.0 [68]. “SMPL” denotes requiring ground-truth SMPL annotation for model training. “3D Scan” denotes requiring ground-truth scan-level supervision for model training.

| Algorithm | SMPL /3D Scan | PSNR \uparrow | SSIM \uparrow | LPIPS \downarrow |
|-----------|---------------|-----------------|-----------------|--------------------|
| PIFu [1] | ✓ | 17.11 | .8831 | .1313 |
| GTA [9] | ✓ | 16.27 | .8810 | .1379 |
| SIFU [2] | ✓ | 16.19 | .8783 | .1380 |
| SiTH [10] | ✓ | 15.98 | .8779 | .1383 |
| CHROME | ✗ | 20.54 | .9098 | .0893 |

Quantitative Results: We present a quantitative evaluation of our proposed algorithm, CHROME, against state-of-the-art methods on the artificially occluded THuman2.0 dataset (Table 1), assessing novel view reconstruction quality across 16 viewpoints. CHROME achieves statistically significant improvements over existing approaches [1, 2, 9], which exhibit inconsistent de-occlusion performance, with a notable ≈ 3 dB PSNR gain over PIFu [1]. Further geometric analysis (Table 2) demonstrates CHROME’s superiority,

Table 2. Quantitative comparison for Geometric Reconstruction on Occluded THuman2.0 [68].

| Algorithm | SMPL /3D Scan | CD \downarrow | P2S \downarrow | NC \uparrow |
|-----------|---------------|-----------------|------------------|---------------|
| PIFu [1] | ✓ | 2.744 | 1.766 | 0.582 |
| GTA [9] | ✓ | 3.266 | 1.675 | 0.603 |
| ECON [18] | ✓ | 3.296 | 1.691 | 0.606 |
| SIFU [2] | ✓ | 3.253 | 1.651 | 0.603 |
| SiTH [10] | ✓ | 2.748 | 1.746 | 0.592 |
| CHROME | ✗ | 1.712 | 1.347 | 0.697 |

particularly in preserving surface details under occlusion, with marked margins across all metrics. These results validate CHROME’s robustness in addressing occlusions while maintaining geometric fidelity, outperforming baselines for both photometric and geometric reconstruction.

Table 3. Quantitative comparison for zero-shot novel view texture reconstruction on Occluded CustomHumans [69].

| Algorithm | SMPL /3D Scan | PSNR \uparrow | SSIM \uparrow | LPIPS \downarrow |
|-----------|---------------|-----------------|-----------------|--------------------|
| PIFu [1] | ✓ | 14.77 | .8779 | .1353 |
| GTA [9] | ✓ | 13.90 | .8955 | .1274 |
| SIFU [2] | ✓ | 13.93 | .8939 | .1273 |
| SiTH [10] | ✓ | 13.87 | 0.8959 | .1284 |
| CHROME | ✗ | 18.54 | .9130 | .0850 |

In Tables 3 and 4, we present **zero-shot generalization** ability of CHROME on artificially occluded CustomHumans [69] dataset in terms of occlusion-free novel view synthesis across 16 views and geometric reconstruction. Clearly, CHROME comfortably outperforms all baseline algorithms [1, 2, 9, 10, 18]. Finally, in Table 5, we present the **zero-shot generalization** capacity of CHROME on the AHP [11] dataset, where CHROME demonstrates superior performance compared to existing baselines. For the naturally occluded AHP dataset, due to the absence of multi-view ground truths, we evaluate results for input-view



Figure 4. **Qualitative analysis of CHROME on artificially occluded THuman2.0 and CustomHumans:** Qualitative results of CHROME against state-of-the-art algorithms [1, 2, 9, 10] on artificially occluded THuman2.0 (top three rows) and artificially occluded CustomHumans (bottom three rows); clearly none of the baseline algorithm perform occlusion-free novel view synthesis whereas CHROME effectively mitigates occlusions and predicts multiview consistent reconstructions.

de-occlusion. In all cases, we observe that the zero-shot generalization performance of CHROME is better than existing algorithms [1, 2, 9, 10, 18].

Qualitative Results: We present qualitative comparisons of CHROME with the baseline algorithms in Figures 4 and 5 in the in-domain artificially occluded datasets THuman2.0 [68], out-of-domain artificially occluded CustomHumans [69] for novel view synthesis and geometric reconstructions via normal maps. These results clearly

show that existing algorithms fail to generate occlusion-free novel views from a single occluded image. Moreover, under occlusions, the generated novel views often suffer from anatomical implausibility and severe multiview inconsistencies. In contrast, CHROME consistently produces novel views that are occlusion-resilient and multiview consistent. This is qualitatively shown for all 16 views in Figure 7. Figure 6 shows the qualitative results of CHROME when stereo inputs are available, showcasing the inherent flexibility of CHROME in generating occlusion-free novel

Table 4. Quantitative comparison for zero-shot Geometric Reconstruction on Occluded CustomHumans [69].

| Algorithm | SMPL /3D Scan | CD ↓ | P2S ↓ | NC ↑ |
|-----------|---------------|--------------|--------------|--------------|
| PIFu [1] | ✓ | 5.751 | 3.679 | 0.621 |
| GTA [9] | ✓ | 8.418 | 2.763 | 0.688 |
| ECON [18] | ✓ | 8.065 | 2.963 | 0.678 |
| SIFU [2] | ✓ | 7.408 | 2.867 | 0.689 |
| SiTH [10] | ✓ | 7.783 | 2.985 | 0.675 |
| CHROME | ✗ | 4.142 | 2.392 | 0.748 |

Table 5. Quantitative comparison for zero-shot Input View Texture Reconstruction on AHP [11].

| Algorithm | SMPL /3D Scan | PSNR ↑ | SSIM ↑ | LPIPS ↓ |
|-----------|---------------|--------------|--------------|--------------|
| PIFu [1] | ✓ | 14.88 | .8317 | .1620 |
| GTA [9] | ✓ | 13.64 | .8234 | .1754 |
| SIFU [2] | ✓ | 13.71 | .8248 | .1727 |
| SiTH [10] | ✓ | 13.44 | .8336 | .1706 |
| CHROME | ✗ | 17.77 | .8558 | .1296 |

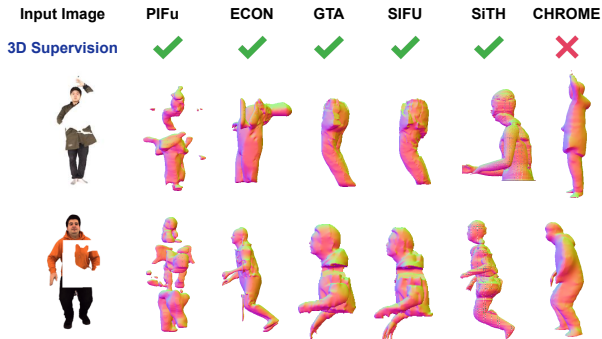


Figure 5. **Qualitative analysis of geometric reconstruction via normal maps:** Qualitative comparisons of CHROME against state-of-the-art methods for geometric reconstruction via normal consistency. Clearly, the predictions from existing algorithms are not occlusion-resilient, generating implausible reconstructions whereas CHROME effectively handles occlusions, producing occlusion-resilient reconstructions.

views under stereo reconstruction settings.

How Robust are Existing Large Reconstruction Models for Occlusion-Free Novel View Synthesis? We showcase qualitative comparisons with three baseline algorithms: Zero123++ [23], ImageDream with LGM [61], and SV3D [72], utilizing their pretrained weights for the task of occlusion-free novel view reconstruction in Figure 8. The



Figure 6. **Stereo Reconstruction:** Visual outcomes of CHROME utilizing stereo occluded images of the same human.

results reveal significant inconsistencies in these existing methods when applied to our task, underscoring the need for a specialized algorithm CHROME.

Ablation Study: Table 6 highlights the importance of incorporating the estimated 3D pose [35] from the occluded image as an explicit guidance signal for our multiview diffusion model, \mathcal{F}_D , on the occluded THuman2.0 dataset [68]. In particular, even without using the estimated 3D pose as conditioning information, CHROME outperforms existing baselines as shown in Table 1. However, integrating the pose as explicit guidance leads to more anatomically accu-

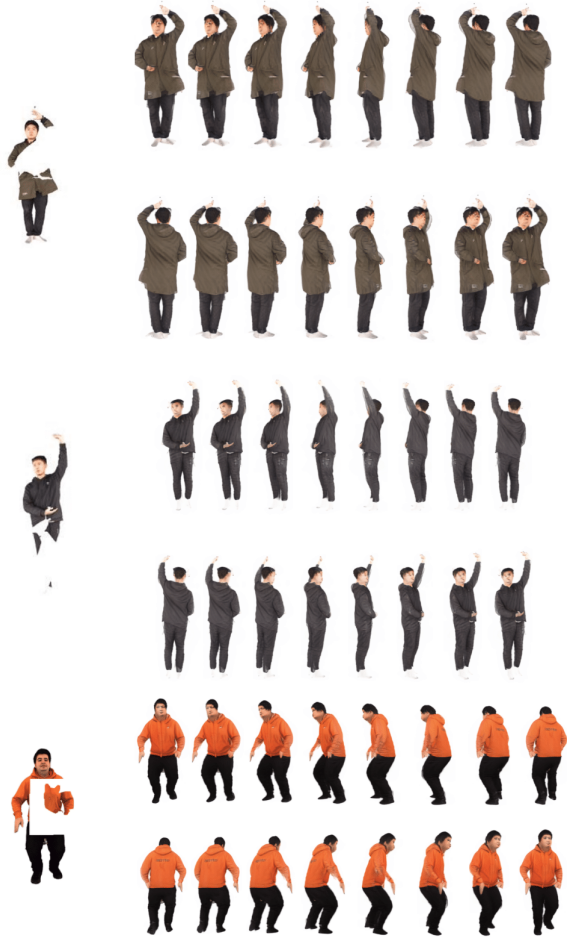


Figure 7. **Visual Results of CHROME on occluded THuman2.0 and CustomHumans:** Qualitative results of CHROME on occluded THuman2.0 and occluded CustomHumans.

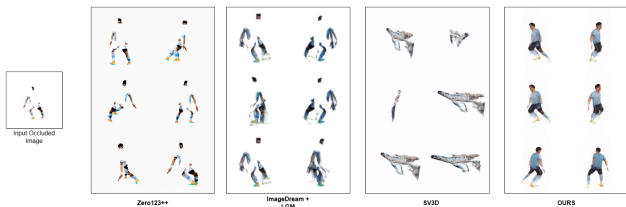


Figure 8. Comparative Qualitative Analysis of Existing Large Reconstruction Models for Zero-Shot Novel View Texture Reconstruction from Occluded Single View Images.

rate reconstructions.

5. Conclusion

We introduce CHROME, a novel two-stage algorithm designed for occlusion-resistant, multiview-consistent 3D reconstruction of clothed humans from a single occluded im-

Table 6. Ablation study on the effect of using estimated 3D pose [35] as an explicit pose conditioning on occluded Thuman2.0. Note that, even without using any pose guidance, we outperform baseline algorithms in Table 1.

| Method | PSNR \uparrow | SSIM \uparrow | LPIPS \downarrow |
|-----------------------|-----------------|-----------------|--------------------|
| CHROME w/o pose cond. | 20.40 | .8833 | .0966 |
| CHROME | 20.54 | .9098 | .0893 |

age. Using a pose-controlled diffusion model to generate occlusion-free images and a 3D reconstruction model conditioned on both the initial occluded image and the synthesized multiview images, CHROME effectively captures and integrates geometric and texture details across multiple views. This approach ensures robust multiview reconstruction under occlusions, overcoming the limitations of existing methods. The experimental results on challenging datasets demonstrate the superiority of CHROME in producing novel view synthesis and geometric reconstructions that are both occlusion resilient and multiview consistent, marking a significant advancement in the field of 3D reconstruction from occluded images.

References

- [1] Shunsuke Saito, Zeng Huang, Ryota Natsume, Shigeo Morishima, Angjoo Kanazawa, and Hao Li. Pifu: Pixel-aligned implicit function for high-resolution clothed human digitization. In *Proceedings of the IEEE/CVF International Conference on Computer Vision (ICCV)*, pages 2304–2314, 2019. 1, 2, 3, 6, 7, 8
- [2] Zechuan Zhang, Zongxin Yang, and Yi Yang. Sifu: Side-view conditioned implicit function for real-world usable clothed human reconstruction. In *Proceedings of the IEEE/CVF Conference on Computer Vision and Pattern Recognition*, pages 9936–9947, 2024. 1, 2, 3, 6, 7, 8
- [3] Song-Hai Zhang, Ruilong Li, Xin Dong, Paul Rosin, Zixi Cai, Xi Han, Dingcheng Yang, Haozhi Huang, and Shi-Min Hu. Pose2seg: Detection free human instance segmentation. In *Proceedings of the IEEE/CVF conference on computer vision and pattern recognition*, pages 889–898, 2019. 1
- [4] Shunyuan Zheng, Boyao Zhou, Ruizhi Shao, Boning Liu, Shengping Zhang, Liqiang Nie, and Yebin Liu. Gps-gaussian: Generalizable pixel-wise 3d gaussian splatting for real-time human novel view synthesis. In *Proceedings of the IEEE/CVF Conference on Computer Vision and Pattern Recognition*, pages 19680–19690, 2024. 1, 5
- [5] Chung-Yi Weng, Brian Curless, Pratul P Srinivasan, Jonathan T Barron, and Ira Kemelmacher-Shlizerman. Humannerf: Free-viewpoint rendering of moving people from monocular video. In *Proceedings of the IEEE/CVF conference on computer vision and pattern Recognition*, pages 16210–16220, 2022. 1, 2, 3
- [6] Matur Rahman Minar, Thai Thanh Tuan, Heejune Ahn, Paul Rosin, and Yu-Kun Lai. 3d reconstruction of clothes using

- a human body model and its application to image-based virtual try-on. In *Proc. IEEE/CVF Conf. Comput. Vis. Pattern Recognit.(CVPR) Workshops*, 2020. 1
- [7] Xuanmeng Zhang, Jianfeng Zhang, Rohan Chacko, Hongyi Xu, Guoxian Song, Yi Yang, and Jiashi Feng. Getavatar: Generative textured meshes for animatable human avatars. In *Proceedings of the IEEE/CVF International Conference on Computer Vision*, pages 2273–2282, 2023. 1
- [8] Shunsuke Saito, Tomas Simon, Jason Saragih, and Hanbyul Joo. Pifuhd: Multi-level pixel-aligned implicit function for high-resolution 3d human digitization. In *Proceedings of the IEEE/CVF Conference on Computer Vision and Pattern Recognition (CVPR)*, pages 84–93, 2020. 2, 3
- [9] Zechuan Zhang, Li Sun, Zongxin Yang, Ling Chen, and Yi Yang. Global-correlated 3d-decoupling transformer for clothed avatar reconstruction. *Advances in Neural Information Processing Systems*, 36, 2024. 2, 3, 6, 7, 8
- [10] I Ho, Jie Song, Otmar Hilliges, et al. Sith: Single-view textured human reconstruction with image-conditioned diffusion. In *Proceedings of the IEEE/CVF Conference on Computer Vision and Pattern Recognition*, pages 538–549, 2024. 2, 3, 4, 6, 7, 8
- [11] Qiang Zhou, Shiyin Wang, Yitong Wang, Zilong Huang, and Xinggang Wang. Human de-occlusion: Invisible perception and recovery for humans. In *Proceedings of the IEEE/CVF Conference on Computer Vision and Pattern Recognition*, pages 3691–3701, 2021. 2, 5, 6, 8
- [12] Adam Sun, Tiange Xiang, Scott Delp, Li Fei-Fei, and Ehsan Adeli. Occfusion: Rendering occluded humans with generative diffusion priors. *arXiv preprint arXiv:2407.00316*, 2024. 2, 3
- [13] Arindam Dutta, Rohit Lal, Dripta S Raychaudhuri, Calvin-Khang Ta, and Amit K Roy-Chowdhury. Poise: Pose guided human silhouette extraction under occlusions. In *Proceedings of the IEEE/CVF Winter Conference on Applications of Computer Vision*, pages 6153–6163, 2024. 2
- [14] Ting Liu, Jennifer J Sun, Long Zhao, Jiaping Zhao, Liangzhe Yuan, Yuxiao Wang, Liang-Chieh Chen, Florian Schroff, and Hartwig Adam. View-invariant, occlusion-robust probabilistic embedding for human pose. *International Journal of Computer Vision*, 130(1):111–135, 2022. 2
- [15] Yi Zhang, Pengliang Ji, Angtian Wang, Jieru Mei, Adam Kortylewski, and Alan Yuille. 3d-aware neural body fitting for occlusion robust 3d human pose estimation. In *Proceedings of the IEEE/CVF International Conference on Computer Vision*, pages 9399–9410, 2023. 2
- [16] Matthew Loper, Naureen Mahmood, Javier Romero, Gerard Pons-Moll, and Michael J Black. Smpl: A skinned multi-person linear model. In *Seminal Graphics Papers: Pushing the Boundaries, Volume 2*, pages 851–866. 2023. 2
- [17] Yuliang Xiu, Jinlong Yang, Dimitrios Tzionas, and Michael J Black. Icon: Implicit clothed humans obtained from normals. In *2022 IEEE/CVF Conference on Computer Vision and Pattern Recognition (CVPR)*, pages 13286–13296. IEEE, 2022. 2, 3
- [18] Yuliang Xiu, Jinlong Yang, Xu Cao, Dimitrios Tzionas, and Michael J Black. Econ: Explicit clothed humans optimized via normal integration. In *Proceedings of the IEEE/CVF conference on computer vision and pattern recognition*, pages 512–523, 2023. 2, 3, 6, 7, 8
- [19] Ben Mildenhall, Pratul P Srinivasan, Matthew Tancik, Jonathan T Barron, Ravi Ramamoorthi, and Ren Ng. Nerf: Representing scenes as neural radiance fields for view synthesis. *Communications of the ACM*, 65(1):99–106, 2021. 2, 3
- [20] Bernhard Kerbl, Georgios Kopanas, Thomas Leimkühler, and George Drettakis. 3d gaussian splatting for real-time radiance field rendering. *ACM Transactions on Graphics*, 42(4), July 2023. 2, 3, 5
- [21] Shoukang Hu, Tao Hu, and Ziwei Liu. Gauhuman: Articulated gaussian splatting from monocular human videos. In *Proceedings of the IEEE/CVF Conference on Computer Vision and Pattern Recognition*, pages 20418–20431, 2024. 2, 3
- [22] Tiange Xiang, Adam Sun, Jiajun Wu, Ehsan Adeli, and Li Fei-Fei. Rendering humans from object-occluded monocular videos. In *Proceedings of the IEEE/CVF International Conference on Computer Vision*, pages 3239–3250, 2023. 2, 3
- [23] Ruoxi Shi, Hansheng Chen, Zhuoyang Zhang, Minghua Liu, Chao Xu, Xinyue Wei, Linghao Chen, Chong Zeng, and Hao Su. Zero123++: a single image to consistent multi-view diffusion base model. *arXiv preprint arXiv:2310.15110*, 2023. 2, 3, 4, 8
- [24] Zerong Zheng, Tao Yu, Yebin Liu, and Qionghai Dai. Pamir: Parametric model-conditioned implicit representation for image-based human reconstruction. *IEEE transactions on pattern analysis and machine intelligence*, 44(6):3170–3184, 2021. 2, 3
- [25] Angjoo Kanazawa, Michael J Black, David W Jacobs, and Jitendra Malik. End-to-end recovery of human shape and pose. In *Proceedings of the IEEE conference on computer vision and pattern recognition*, pages 7122–7131, 2018. 2
- [26] Federica Bogo, Angjoo Kanazawa, Christoph Lassner, Peter Gehler, Javier Romero, and Michael J Black. Keep it smpl: Automatic estimation of 3d human pose and shape from a single image. In *Computer Vision—ECCV 2016: 14th European Conference, Amsterdam, The Netherlands, October 11–14, 2016, Proceedings, Part V 14*, pages 561–578. Springer, 2016. 2
- [27] Hanbyul Joo, Natalia Neverova, and Andrea Vedaldi. Exemplar fine-tuning for 3d human model fitting towards in-the-wild 3d human pose estimation. In *2021 International Conference on 3D Vision (3DV)*, pages 42–52. IEEE, 2021. 2
- [28] Gyeongsik Moon and Kyoung Mu Lee. I2l-meshnet: Image-to-lixel prediction network for accurate 3d human pose and mesh estimation from a single rgb image. In *Computer Vision—ECCV 2020: 16th European Conference, Glasgow, UK, August 23–28, 2020, Proceedings, Part VII 16*, pages 752–768. Springer, 2020.
- [29] Muhammed Kocabas, Chun-Hao P Huang, Otmar Hilliges, and Michael J Black. Pare: Part attention regressor for 3d human body estimation. In *Proceedings of the IEEE/CVF*

- international conference on computer vision*, pages 11127–11137, 2021.
- [30] Yusuke Yoshiyasu. Deformable mesh transformer for 3d human mesh recovery. In *Proceedings of the IEEE/CVF Conference on Computer Vision and Pattern Recognition*, pages 17006–17015, 2023. 2
- [31] Michael J Black, Priyanka Patel, Joachim Tesch, and Jinlong Yang. Bedlam: A synthetic dataset of bodies exhibiting detailed lifelike animated motion. In *Proceedings of the IEEE/CVF Conference on Computer Vision and Pattern Recognition*, pages 8726–8737, 2023. 2
- [32] Tsung-Yi Lin, Michael Maire, Serge Belongie, James Hays, Pietro Perona, Deva Ramanan, Piotr Dollár, and C Lawrence Zitnick. Microsoft coco: Common objects in context. *European Conference on Computer Vision*, pages 740–755, 2014. 2
- [33] Mykhaylo Andriluka, Leonid Pishchulin, Peter Gehler, and Bernt Schiele. 2d human pose estimation: New benchmark and state of the art analysis. In *Proceedings of the IEEE Conference on Computer Vision and Pattern Recognition*, pages 3686–3693, 2014.
- [34] Hanbyul Joo, Hao Liu, Lei Tan, Lin Gui, Bart Nabbe, Iain Matthews, Takeo Kanade, Shohei Nobuhara, and Yaser Sheikh. Panoptic studio: A massively multiview system for social motion capture. In *Proceedings of the IEEE international conference on computer vision*, pages 3334–3342, 2015. 2
- [35] Shubham Goel, Georgios Pavlakos, Jathushan Rajasegaran, Angjoo Kanazawa, and Jitendra Malik. Humans in 4d: Reconstructing and tracking humans with transformers. In *Proceedings of the IEEE/CVF International Conference on Computer Vision*, pages 14783–14794, 2023. 2, 4, 8, 9
- [36] Rawal Khirodkar, Shashank Tripathi, and Kris Kitani. Occluded human mesh recovery. In *Proceedings of the IEEE/CVF conference on computer vision and pattern recognition*, pages 1715–1725, 2022. 2
- [37] Tianshu Zhang, Buzhen Huang, and Yangang Wang. Object-occluded human shape and pose estimation from a single color image. In *Proceedings of the IEEE/CVF conference on computer vision and pattern recognition*, pages 7376–7385, 2020.
- [38] Rongyu Chen, Linlin Yang, and Angela Yao. Mhentropy: Entropy meets multiple hypotheses for pose and shape recovery. In *Proceedings of the IEEE/CVF International Conference on Computer Vision*, pages 14840–14849, 2023. 2
- [39] Garvita Tiwari, Dimitrije Antić, Jan Eric Lenssen, Nikolaos Sarafianos, Tony Tung, and Gerard Pons-Moll. Pose-ndf: Modeling human pose manifolds with neural distance fields. In *European Conference on Computer Vision*, pages 572–589. Springer, 2022. 2
- [40] Calvin-Khang Ta, Arindam Dutta, Rohit Kundu, Rohit Lal, Hannah Dela Cruz, Dripta S Raychaudhuri, and Amit Roy-Chowdhury. Multi-modal pose diffuser: A multi-modal generative conditional pose prior. *arXiv preprint arXiv:2410.14540*, 2024. 2
- [41] Shoukang Hu, Fangzhou Hong, Liang Pan, Haiyi Mei, Lei Yang, and Ziwei Liu. Sherf: Generalizable human nerf from a single image. In *Proceedings of the IEEE/CVF International Conference on Computer Vision*, pages 9352–9364, 2023. 3
- [42] Panwang Pan, Zhuo Su, Chenguo Lin, Zhen Fan, Yongjie Zhang, Zeming Li, Tingting Shen, Yadong Mu, and Yebin Liu. Humansplat: Generalizable single-image human gaussian splatting with structure priors. *arXiv preprint arXiv:2406.12459*, 2024. 3
- [43] Yangyi Huang, Hongwei Yi, Yuliang Xiu, Tingting Liao, Jiaxiang Tang, Deng Cai, and Justus Thies. Tech: Text-guided reconstruction of lifelike clothed humans. In *2024 International Conference on 3D Vision (3DV)*, pages 1531–1542. IEEE, 2024. 3
- [44] Junying Wang, Jae Shin Yoon, Tuanfeng Y Wang, Krishna Kumar Singh, and Ulrich Neumann. Complete 3d human reconstruction from a single incomplete image. In *Proceedings of the IEEE/CVF Conference on Computer Vision and Pattern Recognition*, pages 8748–8758, 2023. 3
- [45] Tiange Xiang, Adam Sun, Scott Delp, Kazuki Kozuka, Li Fei-Fei, and Ehsan Adeli. Wild2avatar: Rendering humans behind occlusions. *arXiv preprint arXiv:2401.00431*, 2023. 3
- [46] Robin Rombach, Andreas Blattmann, Dominik Lorenz, Patrick Esser, and Björn Ommer. High-resolution image synthesis with latent diffusion models. In *Proceedings of the IEEE/CVF conference on computer vision and pattern recognition*, pages 10684–10695, 2022. 3, 4
- [47] Ruoshi Liu, Rundi Wu, Basile Van Hoorick, Pavel Tokmakov, Sergey Zakharov, and Carl Vondrick. Zero-1-to-3: Zero-shot one image to 3d object. In *Proceedings of the IEEE/CVF international conference on computer vision*, pages 9298–9309, 2023. 3
- [48] Yichun Shi, Peng Wang, Jianglong Ye, Mai Long, Kejie Li, and Xiao Yang. Mvdream: Multi-view diffusion for 3d generation. *arXiv preprint arXiv:2308.16512*, 2023. 3
- [49] Ruiqi Gao, Aleksander Holynski, Philipp Henzler, Arthur Brussee, Ricardo Martin-Brualla, Pratul Srinivasan, Jonathan T Barron, and Ben Poole. Cat3d: Create anything in 3d with multi-view diffusion models. *arXiv preprint arXiv:2405.10314*, 2024.
- [50] Guocheng Qian, Jinjie Mai, Abdullah Hamdi, Jian Ren, Aliaksandr Siarohin, Bing Li, Hsin-Ying Lee, Ivan Skokhodov, Peter Wonka, Sergey Tulyakov, et al. Magic123: One image to high-quality 3d object generation using both 2d and 3d diffusion priors. *arXiv preprint arXiv:2306.17843*, 2023. 3
- [51] Lvmin Zhang, Anyi Rao, and Maneesh Agrawala. Adding conditional control to text-to-image diffusion models. In *Proceedings of the IEEE/CVF International Conference on Computer Vision*, pages 3836–3847, 2023. 3, 4
- [52] Xuan Ju, Ailing Zeng, Chenchen Zhao, Jianan Wang, Lei Zhang, and Qiang Xu. Humansd: A native skeleton-guided diffusion model for human image generation. In *Proceedings of the IEEE/CVF International Conference on Computer Vision*, pages 15988–15998, 2023. 3
- [53] Yuanxun Lu, Jingyang Zhang, Shiwei Li, Tian Fang, David McKinnon, Yanghai Tsin, Long Quan, Xun Cao, and Yao

- Yao. Direct2. 5: Diverse text-to-3d generation via multi-view 2.5 d diffusion. In *Proceedings of the IEEE/CVF Conference on Computer Vision and Pattern Recognition*, pages 8744–8753, 2024. 3
- [54] Christoph Schuhmann, Romain Beaumont, Richard Vencu, Cade Gordon, Ross Wightman, Mehdi Cherti, Theo Coombes, Aarush Katta, Clayton Mullis, Mitchell Wortsman, et al. Laion-5b: An open large-scale dataset for training next generation image-text models. *Advances in Neural Information Processing Systems*, 35:25278–25294, 2022. 3
- [55] Ben Poole, Ajay Jain, Jonathan T Barron, and Ben Mildenhall. Dreamfusion: Text-to-3d using 2d diffusion. *arXiv preprint arXiv:2209.14988*, 2022. 3
- [56] Jiatao Gu, Alex Trevithick, Kai-En Lin, Joshua M Susskind, Christian Theobalt, Lingjie Liu, and Ravi Ramamoorthi. Nerfdiff: Single-image view synthesis with nerf-guided distillation from 3d-aware diffusion. In *International Conference on Machine Learning*, pages 11808–11826. PMLR, 2023.
- [57] Inhee Lee, Byungjun Kim, and Hanbyul Joo. Guess the unseen: Dynamic 3d scene reconstruction from partial 2d glimpses. In *Proceedings of the IEEE/CVF Conference on Computer Vision and Pattern Recognition*, pages 1062–1071, 2024. 3
- [58] Yicong Hong, Kai Zhang, Jiuxiang Gu, Sai Bi, Yang Zhou, Difan Liu, Feng Liu, Kalyan Sunkavalli, Trung Bui, and Hao Tan. Lrm: Large reconstruction model for single image to 3d. *arXiv preprint arXiv:2311.04400*, 2023. 3
- [59] Matt Deitke, Dustin Schwenk, Jordi Salvador, Luca Weihs, Oscar Michel, Eli VanderBilt, Ludwig Schmidt, Kiana Ehsani, Aniruddha Kembhavi, and Ali Farhadi. Objaverse: A universe of annotated 3d objects. *arXiv preprint arXiv:2212.08051*, 2022. 3, 4
- [60] Matt Deitke, Ruoshi Liu, Matthew Wallingford, Huong Ngo, Oscar Michel, Aditya Kusupati, Alan Fan, Christian Laforte, Vikram Voleti, Samir Yitzhak Gadre, Eli VanderBilt, Aniruddha Kembhavi, Carl Vondrick, Georgia Gkioxari, Kiana Ehsani, Ludwig Schmidt, and Ali Farhadi. Objaverse-xl: A universe of 10m+ 3d objects. *arXiv preprint arXiv:2307.05663*, 2023. 3
- [61] Jiaxiang Tang, Zhaoxi Chen, Xiaokang Chen, Tengfei Wang, Gang Zeng, and Ziwei Liu. Lgm: Large multi-view gaussian model for high-resolution 3d content creation. In *European Conference on Computer Vision*, pages 1–18. Springer, 2024. 3, 5, 8
- [62] Hengrun Zhao, Yu Zeng, Huchuan Lu, and Lijun Wang. Large occluded human image completion via image-prior cooperating. In *Proceedings of the AAAI Conference on Artificial Intelligence*, volume 38, pages 7469–7477, 2024. 4
- [63] Kaiming He, Xinlei Chen, Saining Xie, Yanghao Li, Piotr Dollár, and Ross Girshick. Masked autoencoders are scalable vision learners. In *Proceedings of the IEEE/CVF conference on computer vision and pattern recognition*, pages 16000–16009, 2022. 4
- [64] Jonathan Ho, Ajay Jain, and Pieter Abbeel. Denoising diffusion probabilistic models. *Advances in neural information processing systems*, 33:6840–6851, 2020. 4
- [65] Yinghao Xu, Hao Tan, Fujun Luan, Sai Bi, Peng Wang, Jiahao Li, Zifan Shi, Kalyan Sunkavalli, Gordon Wetzstein, Zexiang Xu, et al. Dmv3d: Denoising multi-view diffusion using 3d large reconstruction model. *arXiv preprint arXiv:2311.09217*, 2023. 5
- [66] Stanislaw Szymanowicz, Christian Rupprecht, and Andrea Vedaldi. Splatter image: Ultra-fast single-view 3d reconstruction. In *Proceedings of the IEEE/CVF Conference on Computer Vision and Pattern Recognition*, pages 10208–10217, 2024. 5
- [67] Richard Zhang, Phillip Isola, Alexei A Efros, Eli Shechtman, and Oliver Wang. The unreasonable effectiveness of deep features as a perceptual metric. In *Proceedings of the IEEE conference on computer vision and pattern recognition*, pages 586–595, 2018. 5, 6
- [68] Tao Yu, Zerong Zheng, Kaiwen Guo, Pengpeng Liu, Qionghai Dai, and Yebin Liu. Function4d: Real-time human volumetric capture from very sparse consumer rgbd sensors. In *IEEE Conference on Computer Vision and Pattern Recognition (CVPR2021)*, June 2021. 5, 6, 7, 8
- [69] Hsuan-I Ho, Lixin Xue, Jie Song, and Otmar Hilliges. Learning locally editable virtual humans. In *Proceedings of the IEEE/CVF Conference on Computer Vision and Pattern Recognition*, pages 21024–21035, 2023. 5, 6, 7, 8
- [70] Qianli Ma, Jinlong Yang, Anurag Ranjan, Sergi Pujades, Gerard Pons-Moll, Siyu Tang, and Michael J. Black. Learning to dress 3d people in generative clothing. In *Computer Vision and Pattern Recognition (CVPR)*, June 2020. 5
- [71] Zhou Wang, Alan C Bovik, Hamid R Sheikh, and Eero P Simoncelli. Image quality assessment: from error visibility to structural similarity. *IEEE transactions on image processing*, 13(4):600–612, 2004. 6
- [72] Vikram Voleti, Chun-Han Yao, Mark Boss, Adam Letts, David Pankratz, Dmitry Tochilkin, Christian Laforte, Robin Rombach, and Varun Jampani. Sv3d: Novel multi-view synthesis and 3d generation from a single image using latent video diffusion. In *European Conference on Computer Vision*, pages 439–457. Springer, 2025. 8